2013-09-06

Numerical and physical modelling of extreme wave impacts on a stationary truncated circular cylinder

Ransley, E

Numerical and Physical Modelling of Extreme Wave Impacts on a Fixed Truncated Circular Cylinder

E. Ransley[#1], M. Hann[#2], D. Greaves[#3], A. Raby[#4], D. Simmonds[#5]

[#]*School of Marine Science and Engineering, Plymouth University*
Drakes Circus, Plymouth, UK

[1]edward.ransley@plymouth.ac.uk

[2]martyn.hann@ plymouth.ac.uk

[3]deborah.greaves@plymouth.ac.uk

[4]alison.raby@plymouth.ac.uk

[5]d.simmonds@ plymouth.ac.uk

Abstract— **With a history of international failures, the survival envelope for wave energy convertors (WECs) has become an important consideration in the design of such systems. Potential design solutions require a better understanding of the hydrodynamics and structural loading experienced during extreme events, like rogue wave impact. This paper concerns the numerical modelling and experimental validation of extreme rogue wave interactions with a fixed truncated circular cylinder. Typical extreme waves from the intermediate depth Wave Hub site were produced at 1:30 scale in the COAST Lab Ocean basin at Plymouth University from the 100 year wave statistics using the dispersive focussing method, NewWave. A fixed 0.4m diameter cylinder with a 0.4m draft was used to represent the geometry of a generic point-absorber type WEC. Physical conditions were duplicated in a numerical wave tank, solving the fully nonlinear Navier-Stokes equations, with a free surface, using the volume of fluid (VoF) method and open source CFD library OpenFOAM®. The comparison between the results shows that the CFD software is capable of simulating extreme wave interactions with a fixed cylinder and the associated hydrodynamic phenomena very well.**

Keywords— **Wave Energy Converter (WEC), survivability, NewWave, OpenFOAM®, waves2Foam, VoF method**

I. INTRODUCTION

For countries with a significant resource, marine renewable energy (MRE) has become a fundamental part of the response to the dual challenges of climate change and energy security. The conversion of wave energy into electricity is one option with great potential and few environmental impacts. Ocean waves have both a high power density and a relatively high utilization factor. However, the wave energy industry is still in the early stages of development and extracting energy from ocean waves has been considered uneconomical due to a lack of good engineering solutions [1, 2]. If, however, economical and technical solutions were developed, the area would have a vast impact on the electricity production in the world [3].

Research directly concerning wave energy converters (WECs) has focussed primarily on optimal response. However, this is not always the most critical factor, in a design context, as highlighted by a history of international WEC and mooring failures. There still exists considerable uncertainty around the prototype behaviour of fully coupled dynamic systems comprising WEC technologies and their moorings. Survivability has now been identified as a key issue for the marine renewables industry posing a significant challenge, requiring complementary development and underpinning research. It is now widely accepted that the current design procedures for the operational envelope must be complimented with a second level of design which considers the survival envelope [4, 5].

In terms of survivability, it is the sometimes catastrophic impacts from abnormally large, 'freak' or 'rogue', waves which are of most concern to WEC developers and the motivation for their investigation. These 'extreme' waves, with amplitudes far exceeding those used to characterise the mean properties and operational conditions of a particular wave field, have received significant attention since 2000 after a few surprising offshore observations [6]. The frequency of incidents involving extreme waves suggests that these events are likely to occur more often and cause more damage than had been thought previously [6].

It is well known that unexpected, large waves can form through refraction in coastal waters or areas with strong currents but there is some debate over how extreme waves are produced in the deep ocean [6]. Many mechanisms have been proposed from linear effects like dispersive focussing to the nonlinear phenomenon known as the Benjamin-Feir, or modulation, instability [7].

Modelling, both physical and numerical, has become increasingly important in the assessment of a given concept before going to the expense of full scale deployment at sea. Developers consider this type of testing to be a vital stage in the engineering development of WECs to ensure the device behaves as expected and no unexpected and costly damage is caused when deployed.

Physical modelling of wave structure interactions, using scale model WECs, in a wave tank, has been widely used by developers. However, for complicated experiments the required analysis can be very difficult, or impossible, as some quantities, like the flow velocity, maybe difficult to measure without disturbing the flow itself.

Continued increases in the performance-to-cost ratio of modern computers has meant that numerical models can now

provide the quantitative description required for engineering analysis more cheaply and simplify the processes of measurement and repeat testing. Furthermore, numerical experiments offer a means to interpret the fundamental phenomenological aspects of experimental conditions that physical tests may not. However, numerical simulations can be extremely time consuming without proper implementation and it is possible for a qualitatively incorrect solution to look reasonable. Without validation from physical tests, the consequences of accepting such a result may be severe [8].

As part of the wider SuperGen UK Centre for Marine Energy Research (UKCMER) project, led by the present authors, entitled 'Survivability of Wave Energy Converter and Mooring coupled system', the aim of this research is to develop a robust combination of, and improve convergence between, experimental measurement techniques and numerical modelling approaches for extreme wave impacts on moored wave energy converters. A fully nonlinear computational fluid dynamics (CFD) approach will be used, validated against experimental and field data, enhancing the design, development and operational efficiency of WEC technologies.

In this preliminary work, extreme wave impacts on a fixed truncated circular cylinder were simulated, both physically and numerically. This geometry was chosen to represent a generic, point-absorber-type WEC and was fixed to simplify the modelling process at this stage. An extreme wave, with a focus location in front of the cylinder, was generated in the physical basin using dispersive focussing. The run-up on the cylinder and a sample of the surrounding surface elevation were measured and compared with the results from the numerical simulation.

II. Background

The continued development of the marine environment has seen the offshore industry spread to deeper water and harsher conditions and the challenge of modelling the interactions between steeper waves and offshore structures has received an increasing amount of attention. Due to the complexities of wave break-up and recombination, wave-structure interactions, run-up and green water effects, the investigation of these phenomena requires a lot of effort.

Typically physical tank testing has been used to model wave-structure interactions. These experiments have the benefit of modelling, and measuring, real hydrodynamics. However, physical models are usually limited by scale restrictions and usually only produce a small data set [9]. In order to overcome these restrictions numerical methods have been developed.

In the past the main focus has been on the diffraction of water waves around a fixed structure, typically using first-order theory in the frequency domain. Second-order [10] and some third order [11] analysis has been developed including time-domain solutions, but these methods are typically limited to waves with low steepness and have limited applications as water waves are fully nonlinear and unsteady. Potential flow methods are used extensively in offshore engineering. These methods involve a model discretised into boundary elements or panels on which the pressure and velocity potential are calculated [12]. These methods are efficient for linear and weakly nonlinear wave-structure interactions but are typically restricted to non-breaking waves [9].

In the last few decades, fully nonlinear numerical wave tank (NWT) models have been developed to investigate cases from nonlinear wave diffraction around offshore structures to three-dimensional overturning waves and violent body motion [10]. So called, Computational Fluid Dynamics (CFD) methods have the advantage, in principle, of being valid for all flow regimes, unlike empirical methods such as the application of the Morrison equation for the forces on a pile. CFD has also been shown to cope with highly distorted flows including wave breaking and recombination [13]. Furthermore, CFD is not restricted to the scales necessary for physical experiments, although they are often validated against such results due to a lack of available full scale data [9].

The classic case of wave interaction with a vertical cylinder has received more and more attention due to the continued development of the oil and gas industry and, more recently, the offshore wind industry with the majority of today's offshore wind turbines being placed on monopile foundations. Numerous physical experiments of wave interactions with various cylinder types have been under taken and form the basis for validation of many numerical modelling methods [14]. There are many studies investigating the highly nonlinear interactions between bottom mounted cylinders and waves from regular to directionally focused waves. The main focus is usually on horizontal forces, run-up and overturning [9, 15-17]. In terms of simple WECs, highly nonlinear wave interactions with floating bodies have received less attention due to the complexity in modelling the fully coupled dynamic behaviour and, for those who have tried, the motion of the object is usually restricted to a single degree of freedom [18].

III. Experimental Method

A. Generation of an Extreme Wave (NewWave)

In order to generate extreme waves, the NewWave formulation of Tromans et al. (1991) was used [19]. The concept of the NewWave formulation is to create an extreme wave at a specific location in space and time via the dispersive focussing of several small waves of different frequencies and deterministically chosen phases. NewWave is a compact wave packet with a local time history identical to the Fourier transform of the spectrum of a sea state and has been used as a design wave in the offshore industry as well as a method for generating extreme waves in numerous experimental and numerical studies [9, 10, 20, 21].

To place this work in the context of a real wave energy project, the 100 year return wave with a crest height of 13.4m, based on a modelled JONSWAP spectrum (H_s =14.4m and T_z = 14.1s) for the Wave Hub site, was used as the extreme wave in the experiments [21]. Located in south-west UK, in water depths of 50-60m, Wave Hub offers offshore infrastructure for the demonstration and proving of pre-commercial wave energy device arrays. The aim of the project is to provide a

link between the full-scale testing of wave energy converters and the deployment of commercial wave energy arrays [22].

As an initial stage to this work, the extreme wave was generated at 1:30 scale in the absence of a cylinder. The water depth was set to 1.73m so that it was correctly scaled to the Wave Hub site (52m) and 243 linear wave components ranging between 0.1 and 2Hz were used to generate the NewWave. This process is the same as that used by Vyzikas et al. [23] and was crucial to ensure that a true focus, defined to be when all components are in phase and the wave packet is symmetrical, was achieved in the physical basin [24]. It also served as an initial validation case for the numerical wave tank used and the results are shown in section five.

B. *Physical Experiments*

The physical experiments were performed in the new Plymouth University COAST laboratory Ocean basin. This is a 35m x 15.5m tank with a raiseable floor of maximum depth 3.0m and 24 flap-type wave paddles. A 0.4m diameter circular cylinder was fixed to the gantry above the tank, with a draft of 0.4m. A set of calibrated resistive wave gauges were positioned in the vicinity of the cylinder (Figure 1) in order to measure a representation of the free surface and the run-up on the upstream side of the cylinder. An additional wave gauge was positioned 8.2m upstream of the centre of the cylinder and the data recorded there used as the input for the numerical models [23]. An accelerometer was installed in the base of the cylinder to measure any motion experienced and to assess to what degree the cylinder was truly stationary. The long crested wave was generated across the entire width of the Ocean basin with the focus location positioned 1.2m in upstream of the cylinder centre. The experiment was repeated, and measurements taken, three times to assess the quality of the experimental data. Furthermore, a ruler was installed inside the transparent cylinder and a video camera mounted to record the run-up on the cylinder. This served as a way to check the measured run-up as the closest wave gauge could not be installed directly on the cylinder surface.

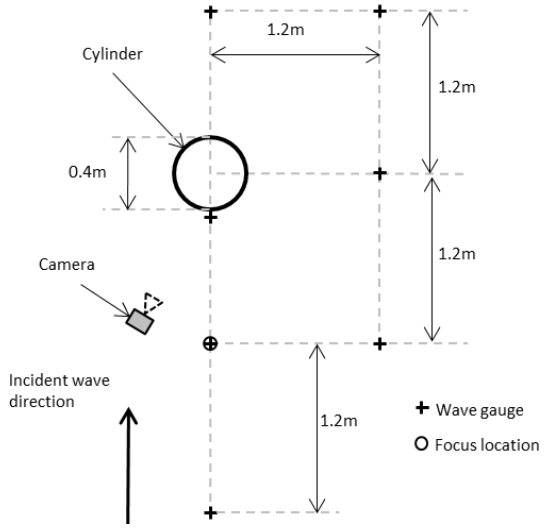

Fig. 1 Schematic of the wave gauge positions and wave focus location used in the main physical experiments relative to the cylinder location

IV. NUMERICAL METHOD

A. *Software*

Corresponding numerical simulations were performed using the Open Source Field Operation and Manipulation (OpenFOAM®) C++ library. The freely available Reynolds averaged Navier-Stokes (RANS) solver for the combined flow of air and water, interFoam, was used to solve for the two immiscible fluids simultaneously, in a numerical wave tank, using the finite volume method and a volume of fluid (VoF), surface capturing approach similar to that of Hirt and Nichols [25]. The VoF method has been selected for this project based on its proven ability to cope with highly deformed free surfaces and topological changes such as wave breaking and recombination [13]. In addition, the wave generation toolbox, waves2Foam, was utilised to generate the numerical NewWave input and remove unwanted reflections from within the numerical wave tank. A more comprehensive description of the solver and the waves2Foam toolbox can be found in Jacobsen et al. [26].

B. *Numerical Simulation of Extreme Waves*

As mentioned above, the initial step in this work was to generate the extreme wave in the absence of a cylinder. This served two purposes; to ensure a true focus was being achieved and to provide an initial validation test for the numerical wave tank.

In order to numerically model the extreme wave a two-dimensional numerical wave tank was constructed. The computational domain was discretised into 71,250 cells in 4 blocks. A global coordinate system was defined with the origin at the still water level and the x-axis pointing in the direction of wave propagation. In the vertical direction, a relatively coarse grid was specified near the sea bed and on the upper boundary, while the region from z = -0.3 m to z = 0.5m (which contains the free-surface) has a uniform, square-celled mesh at a finer resolution. The grid spacing was uniform in the horizontal direction apart from near the inlet boundary where a very fine mesh was specified. This mesh resolution had previously been found to be convergent for the cases used here. A no-slip boundary condition was applied at the sea bed and an outlet condition that allows air to both enter and leave the domain was applied on the top boundary.

The computational domain was 25m long and 1.73m deep and was designed to match the central part of the physical domain. The inlet boundary was located at the position of the upstream wave gauge (8.2m before the cylinder centre) thus allowing the physical result recorded there to be used as the inlet boundary condition in the computational simulations. The amplitudes and phase angles of 243 wave components, with frequencies evenly spaced between 0.008 and 1.89Hz, were derived by means of a fast Fourier transform (FFT) of the time series recorded at the upstream wave gauge during the physical experiments. On the inlet boundary, the second order wave definition given by Sharma and Dean [26] was used to define the amplitude and velocities for each component to avoid the generation of spurious long waves when a linear inlet boundary condition is enforced [16, 28, 29].

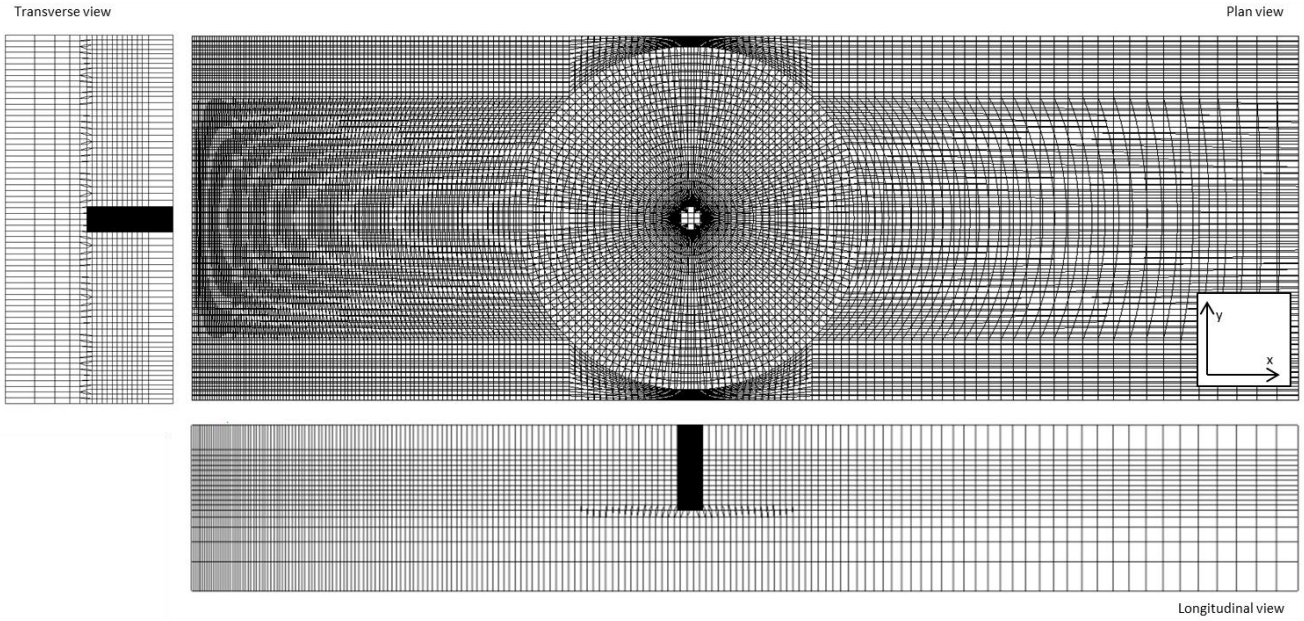

Fig. 2 Representation of the numerical mesh used in the main simulations. Here each cell represents 27 (3x3x3) cells in the mesh used

The incident waves were generated within a 0.1m long relaxation zone in which the wave field was enforced after every time step using an update formula [16, 26]. Finally, another relaxation zone with a target solution of still water was located between x = 12 m and x = 25 m in order to absorb the waves. The adjustable time step function supplied with OpenFOAM® was used with a maximum Courant number of 0.5. No turbulence model was used as turbulence is not expected to have a significant affect in the wave only case.

C. Numerical Simulation of Wave Interaction with a Cylinder

For the main simulations, involving the fixed cylinder, the computational domain was extended to three dimensions. 43 blocks were used to construct a 3D mesh with the cylinder positioned 8.2m from the inlet boundary. The computational domain was 6m wide and 18.2m long. The mesh maintained many of the characteristics of the 2D mesh used above. The still water level was positioned at z=0m and the domain extended from z=-1.73m to z=1m. The mesh was allowed to coarsen towards the top and bottom of the domain and a band of finer cells of constant width was created between z=-0.4m and z=0.5m. Again the mesh was made finer towards the inlet boundary and in order to aid in the absorption of waves towards the outlet zone, the grid was allowed to coarsen towards the end of the domain. A set of blocks surrounding the cylinder were constructed so that the cell size gradually became finer towards the cylinder surface. Figure 2 shows a representation of the mesh used where each cell in the figure represents 27 (3x3x3) cells in the final mesh. 6,022,912 cells were used in total. A zero-velocity wall boundary condition was specified on the cylinder surface and on the sides of the numerical tank. Once again the incident waves were generated within a 0.1m long relaxation zone and a further relaxation zone was located between x=11.2m and x=18.2m. The same input wave definition as above was specified across the entire inlet boundary with the goal of reproducing the results in the physical tank from 8.2m in front of the cylinder. Numerical wave gauges were positioned in the same places as those in the physical tank with the addition of a gauge directly on the upstream face of the cylinder and gauges on the left-hand side of the cylinder symmetrical with those on the right.

Particularly after observing the physical experiments, turbulence is expected to play an important role in the modelling of extreme wave interaction with the cylinder. For these preliminary simulations, however, no turbulence model was used. In future work, different turbulence models will be investigated to find the most appropriate scheme for this case.

V. RESULTS AND DISCUSSION

A. Results From the Wave Only Simulations

Figure 3 shows the resultant time series at the focus location, normalised by the theoretical crest height of 0.46m, from the numerical simulation of the extreme wave in the absence of a cylinder. It can be seen that the numerical wave tank performs very well, particularly during the low amplitude beginning of the wave packet. The shape of the extreme wave has been reproduced with very little phase discrepancy; however, there is some loss of symmetry about the focus point. The deep troughs observed in the physical test have not been reproduced as well but the crests, and especially the main crest, are near perfect. Finally, relatively soon after the main crest passes reflections appear to be damaging the results in the numerical tank.

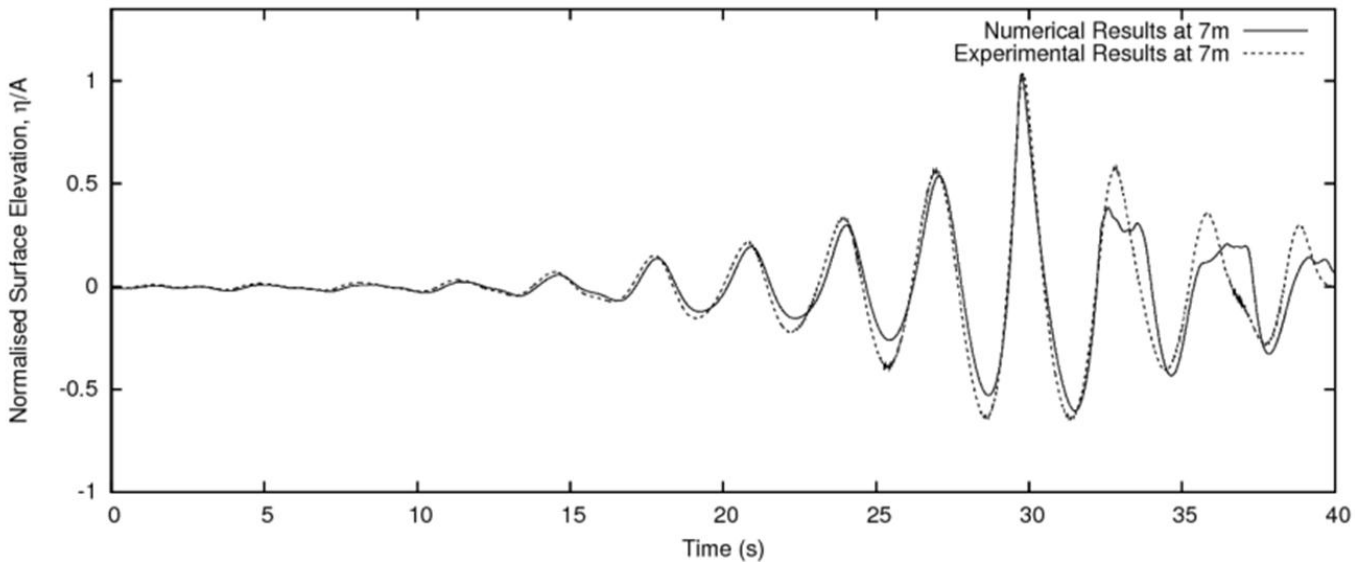

Fig. 3 Time series of the normalized surface elevation for the extreme wave measured at the focus location (7m from the numerical inlet boundary). Dotted line from the physical experiments, solid line from the numerical simulation. The surface elevation is normalized by the theoretical crest height

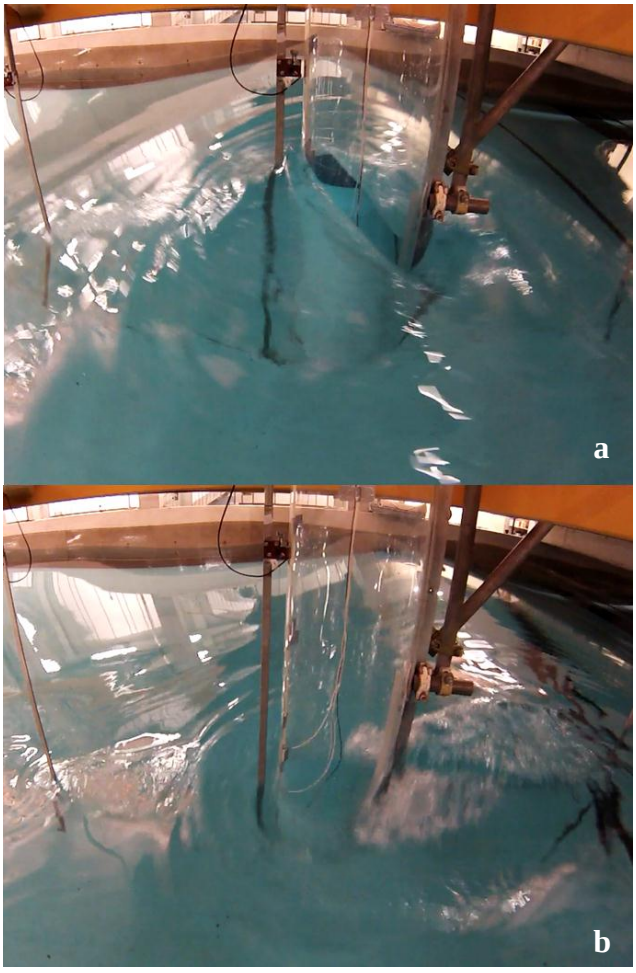

Fig.4 Photographs showing; (a) the moment of maximum run-up, and (b) a broken wave travelling upstream, from behind the cylinder, 0.67s after max. run-up

The reflections observed in the numerical wave tank require further attention, but, altogether it would appear that this methodology and this numerical wave tank approach is capable of simulating the extreme waves required for this project to an acceptable degree.

B. Observations Made During the Physical Experiments

From observations made during the physical experiments and by viewing the videos recorded, a few interesting phenomena have been observed. Until the first of the three main peaks in the wave packet arrives at the cylinder, the free-surface remains smooth, there are no signs of wave scattering or diffraction and the run-up is both in phase and comparable in amplitude to the incident wave. As the higher crests reach the cylinder the difference in surface elevation around the circumference is much greater and some symmetrical scattering of waves is observed in the lee of the cylinder. A well appears behind the cylinder at the same time as a run-up considerably higher than the incident wave is produced. The well is then filled as the free surface collapses backwards towards the cylinder. This causes a spilling broken wave to impact on the rear of the cylinder and propagate upstream moments after the maximum run-up. After the main crest has passed, the free-surface near the cylinder is covered with high frequency disturbances produced by the breaking of this backwards wave. The two images in Figure 4 show this phenomenon. Figure 4a shows the point of maximum run-up for the wave focussed at the cylinder's centre and Figure 4b shows the broken wave at the rear of the cylinder propagating upstream 2/3 of a second later.

C. Main Results

Figure 5 shows the main results for the run-up of the extreme wave on the upstream side of the cylinder. All three

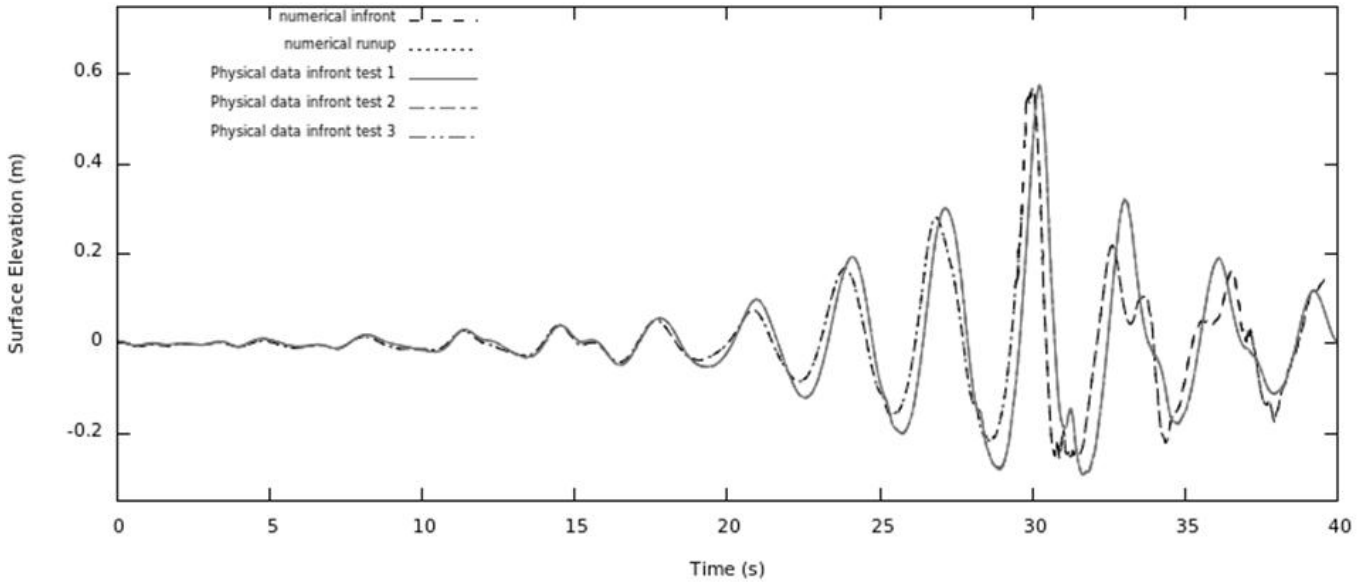

Fig. 5 Times series of the surface elevation recorded just in front of the cylinder during the three repeated physical experiments (grey – 3 lines on top of each other) and during the numerical simulation (black, dashed). Also shown; numerical results for the run-up on the upstream side of the cylinder (black, dotted)

of the physical results, from the wave gauge just in front of the cylinder, are shown in grey. As it can be seen the three physical results are almost identical. This shows that the experimental procedure is robust and repeatable and provides confidence in the quality of the measurements taken.

The peak run-up on the cylinder is 0.575m, 24% greater than the crest height of the wave, however, the shape of the time series measured during the physical experiments is not significantly different to that observed in the absence of the cylinder (Figure 3). The only difference is the small peak immediately after the main peak, at about 31 seconds. This peak is not observed downstream as it can be seen in Figure 6 and is believed to be caused by the broken wave propagating upstream observed in Figure 4b.

Figure 5 also shows the numerical results, in black, at both the position just in front of the cylinder and on the front face of the cylinder itself. These two numerical results are also almost identical suggesting that the run-up jet is sufficiently thick (0.025m+) to register on both wave gauges. This is confirmed in the photograph in Figure 4a which shows the moment of maximum run-up and a relatively wide run-up on the upstream (left) side of the cylinder.

Comparing the physical and numerical results shown in Figure 5; it can be seen that the numerical simulation has produced a very good approximation of the run-up of an extreme wave on a fixed cylinder. Once again the numerical solution is particularly good during the low amplitude part of the wave packet, up until 15 seconds. Again the deep troughs observed in the physical experiments have not been produced as well as hoped but the peaks are very well reproduced. The height of maximum run-up in the numerical simulation is 0.570m, less than 1% smaller than the physical result. Interestingly, there is now some phase discrepancy in the numerical results and the main peaks occur approximately 0.25s earlier than in the physical experiment. There is a hint of the small peak immediately after the main run-up, in the numerical results, but it is not nearly as well pronounced as in the physical results. It is possible that the lack of turbulence modelling applied to the numerical simulation may explain these discrepancies and so will be investigated further in future work. Alternatively, the inevitable motion of the physical cylinder may explain some differences between results with the truly stationary numerical cylinder. Analysis of the accelerometer data, collected during the physical experiments, shows a displacement of ±0.01m (2.5% of the cylinder diameter) at the base of the cylinder which may cause some surface displacement. Finally, Figure 5 again shows that the numerical results appear to be adversely affected by reflections after about 32 seconds. However, observations of the numerical results show that the main crest of the wave packet displays some instability and possible premature breaking resulting in an undulating free-surface following the passing of the main crest (see Figure 7a). This too may be a consequence of using a laminar turbulence scheme (turbulence modelling may be required for the simulation of steep waves) or possibly an issue with the NewWave linear superposition of wave components at the inlet boundary or even a problem with the mesh design (highly non-cubic cells have been seen to produce unreliable results). These variables require further investigation and will be assessed in the future.

Figure 6 shows the complete set of wave gauge measurements recorded during the physical experiment. The plots are arranged according to the wave gauge positions in Figure 1. On the left of the figure the results from the gauges in line with the centre of the cylinder are displayed with the closest gauge to the wave paddles located at the bottom. On

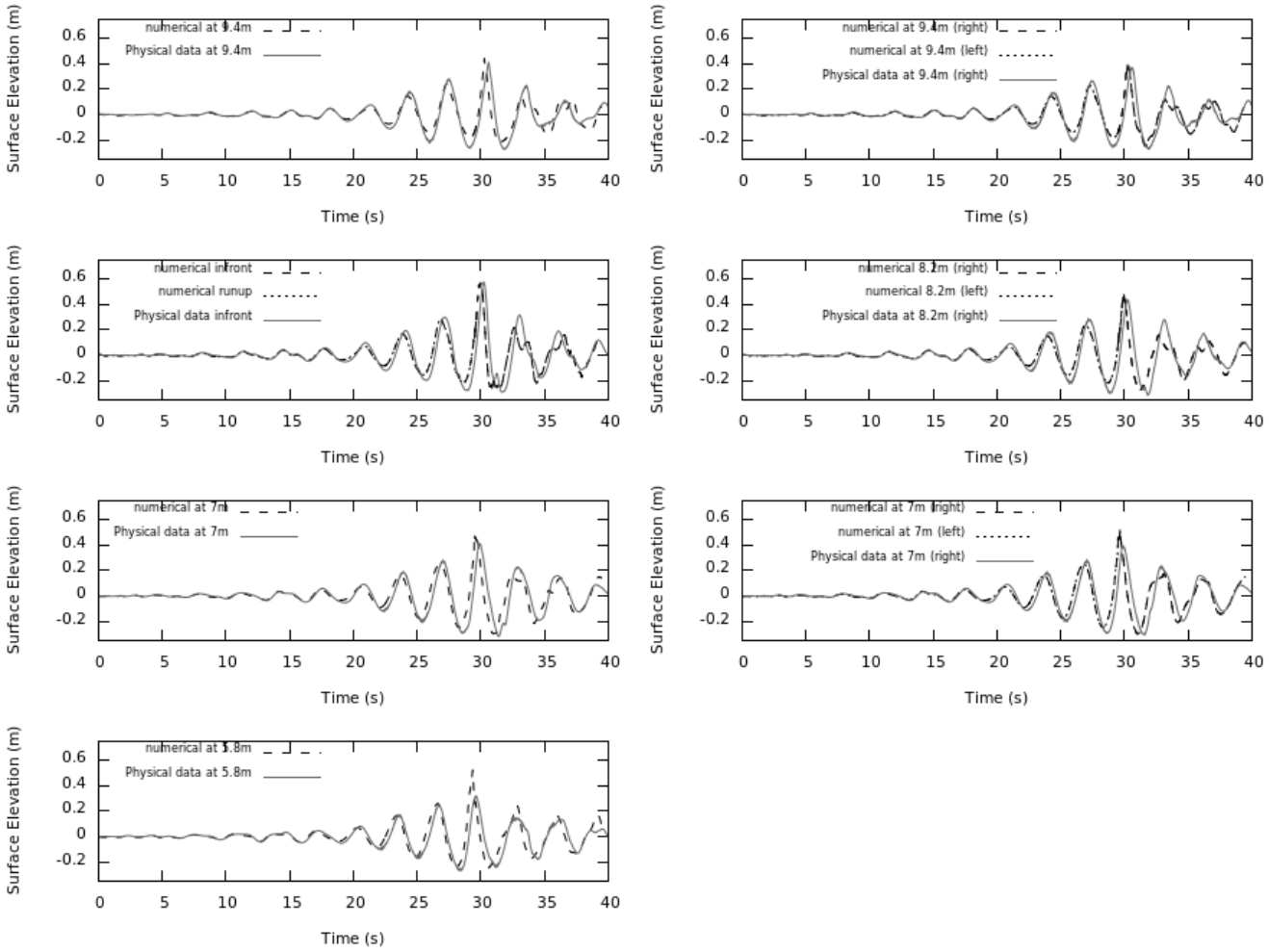

Fig. 6 Time series for the surface elevation recorded at the wave gauge positions in Figure 1. On the left are series from gauges in line with the cylinder centre and on the right are series from the gauges to the right of the cylinder and numerical results from gauges positioned to the left of the cylinder. Physical data is shown as a solid grey line while numerical results are shown in black (dotted or dashed).

the right of the figure are the results from the wave gauges positioned to the right of the cylinder. Also plotted are the numerical results from the same locations in the computational domain with the addition of numerical gauges positioned symmetrically on the left-hand-side of the cylinder (right of Figure 6) to assess the symmetry of the flow around the cylinder and investigate any vortex shedding.

Each of the plots shows similar characteristics to those shown in Figure 5. One difference is that the main crest height observed upstream of the cylinder in the numerical results is significantly greater in amplitude than those recorded in the experiments. Again this may be due to the premature breaking of the numerical wave causing a steepening of the wave crest and numerical breaking close to the inlet boundary.

The extra peak just after the main peak, observed in Figure 5 (also second from top on the left of Figure 6), can also be seen in the time series recorded close to the cylinder but not downstream of it. The further from the cylinder the smaller the extra peak and the later it occurs, consistent with the upstream propagation of the broken wave observed in Figure 4b.

Lastly, the numerical results from the left-hand-side of the cylinder are the same as those recorded to the right (Figure 6 right). This suggests that, in this case, based on the surface elevation, there is no asymmetric vortex shedding. However, the flow structure and the consequences of the factors mentioned above will be analysed further in future work.

Figure 7 shows three surface plots from the numerical simulation at 29.5s (7a), 30s (7b) and 30.5s (7c) with the wave propagating from left to right. Figure 7a shows the undulating surface about the main peak possibly due to premature breaking in the numerical simulation discussed early. Figure 7b shows the moment of maximum run-up. The well behind the cylinder, observed in the physical tests, is clearly visible and the thick run-up jet is similar to that shown in Figure 4a. There is some unusual behaviour of the free surface on the surface of the cylinder with quite a spiky appearance. It is possible that this is a problem with the post-processing programme used or it could be a result of the mesh cells close

to the cylinder becoming very narrow. Both of these possibilities will be investigated further in future work. Figure 7c clearly shows the infilling wave impact on the rear of the cylinder propagating upstream as discussed earlier and shown in Figure 4b. In general, the important hydrodynamic features appear to have been reproduced very well and visually the numerical simulation closely matches the videos taken during the physical experiments.

One of the benefits of CFD is the generation of a large data set which can be used to understand the phenomena present in physical simulations that may not be possible to observe experimentally. Figure 8 shows the velocity vectors at the surface at the time of maximum run-up (8a) and one second later (8b). Figure 8b clearly shows the upstream propagation of the wave created behind the cylinder.

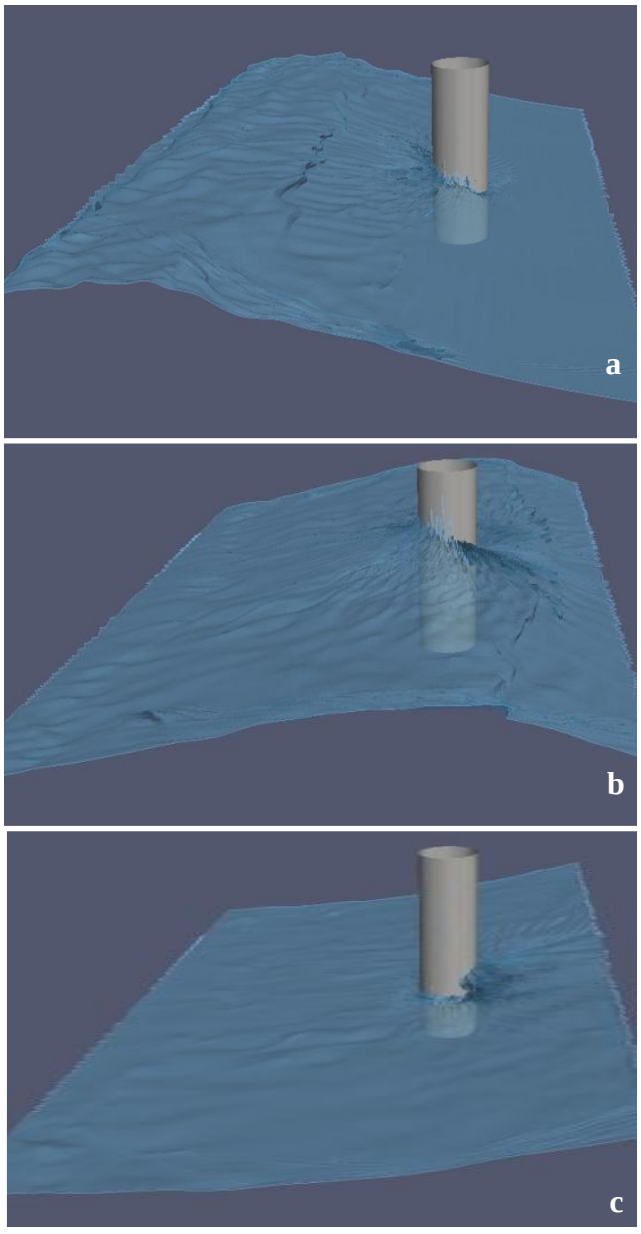

Fig.7 Free surface plots from the numerical simulation at 29.5s (a), 30s (b) and 30.5s (c)

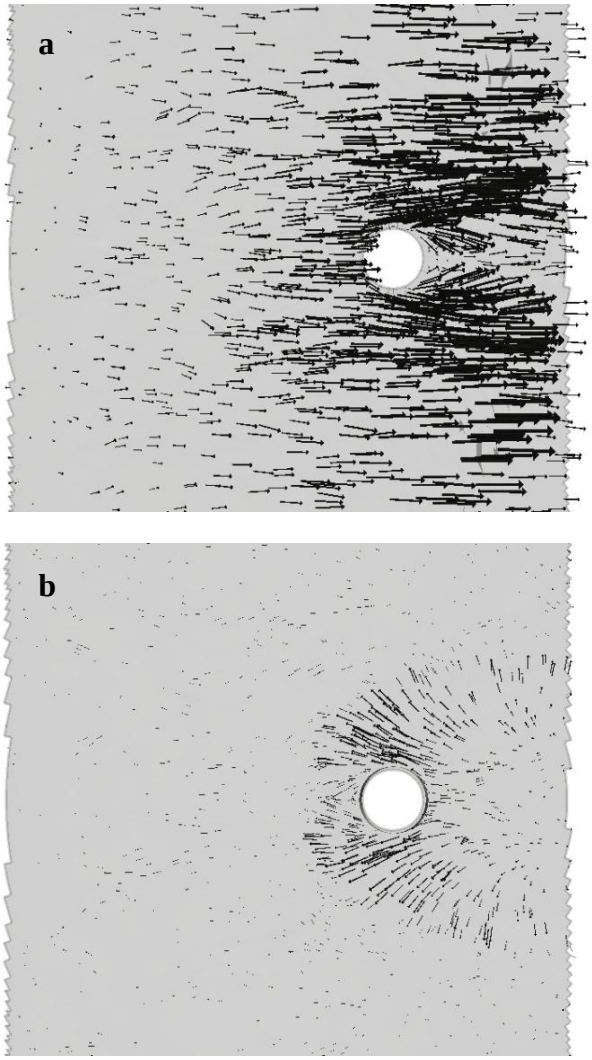

Fig.8 Velocity vectors at the free-surface at the time of maximum run-up (a) and one second later (b)

D. CPU Efficiency

The main model was run using OpenFOAM® 2.1.1 on four Intel® Xeon® CPU E5630 @ 2.53GHz and took over 600 hours to complete the 40s simulation. For this case, parallel processing on only four processors was found to be optimal due to excessive RAM allocation when using more subdomains. Although the VoF method is notoriously CPU intensive, the efficiency of this particular simulation is deemed to be inadequate and further investigation to improve the CPU efficiency is required.

VI. Conclusions

The OpenFOAM® and waves2Foam toolboxes are shown to be able to simulate an extreme wave impact on a circular truncated cylinder and the associated hydrodynamic phenomena comparable to physical results. Further calibration and investigation of various variables, including turbulence modeling, mesh generation and CPU efficiency is planned for future work. The next phase of the project will be to investigate the extreme wave loading on a floating structure.

ACKNOWLEDGMENTS

We would like to thank the OpenFoam users forum for help resolving software implementation issues and Niels Jacobsen for his excellent work developing the waves2foam toolbox.

We would also like to thank the High Powered Computing (HPC) staff at Plymouth University, Peter Mills and Antonio Rago, for technical support and the technical staff of the COAST lab at Plymouth University, Peter Arber and Alistair Reynolds, for their help designing, setting-up and running the experiments.

This project is funded by the EPSRC through SuperGen UK Centre for Marine Energy Research (UKCMER).

REFERENCES

[1] Henfridsson, U., et al., *Wave energy potential in the Baltic Sea and the Danish part of the North Sea, with reflections on the Skagerrak.* Renewable Energy, 2007. **32**(12): p. 2069-2084.

[2] Leijon, M., et al., *An electrical approach to wave energy conversion.* Renewable Energy, 2006. **31**(9): p. 1309-1319.

[3] Leijon, M., et al., *Economical considerations of renewable electric energy production - especially development of wave energy.* Renewable Energy, 2003. **28**(8): p. 1201-1209.

[4] Haver, S. and O.J. Anderson. *Freak Waves: Rare Realization of a Typical Population or Typical Realization of a Rare Population?* in *Proceedings of the 10th International Offshore and polar Engineering Conference (ISOPE)*. 2000. Seattle, USA.

[5] Faulkner, D., *Rogue Waves - Defining their Characteristics for Marine Design*, in *Rogure Waves 2000*. 2000: Brest, France.

[6] Dysthe, K., H.E. Krogstad, and P. Müller, *Rogue waves*, in *Encyclopedia of Ocean Sciences (Second Edition)*, J.H. Steele, K.K. Turekian, and S.A. Thorpe, Editors. 2009, Academic Press: Oxford. p. 770-780.

[7] Clauss, G.F., *Freak Waves and Their Interaction with Ships and Offshore Structures*, in *Advances in Numerical Simulation of Nonlinear Water Waves*, Q. Ma, Editor. 2010, World Scientific Publishing Co. Pte. Ltd. p. 641-689.

[8] Ferziger, J.H. and M. Perić, *Computational Methods for Fluid Dynamics (3rd Edition)*. 2002, Verlag Berlin Heidelberg New York: Springer.

[9] Westphalen, J., et al., *Focused waves and wave-structure interaction in a numerical wave tank.* Ocean Engineering, 2012. **45**: p. 9-21.

[10] Bai, W. and R. Eatock Taylor, *Numerical simulation of fully nonlinear regular and focused wave diffraction around a vertical cylinder using domain decomposition.* Applied Ocean Research, 2007. **29**(1-2): p. 55-71.

[11] Š. Malenica and B. Molin (1995). Third-harmonic wave diffraction by a vertical cylinder. Journal of Fluid Mechanics, 302, pp 203-229.

[12] Newman, J.N. and C.H. Lee, *Boundary-element methods in offshore structural analysis.* Journal of Offshore Mechanics and Arctic Engineering Transactions of the ASME), 2002. **124**(2): p. 81-89.

[13] Greaves, D.M., *Viscous waves and wave-structure interaction in a tank using adapting quadtree grids.* Journal of Fluids and Structures, 2007. **23**(8): p. 1149-1167.

[14] Kriebel, D.L., *Nonlinear wave interaction with a vertical circular cylinder. Part II: Wave run-up.* Ocean Engineering, 1992. **19**(1): p. 75-99.

[15] Christensen, E.D., H. Bredmose, and E.A. Hansen. *Extreme wave forces and run-up on offshore wind turbine foundations*. in *In Proceedings of Copenhagen Offshore Wind*. 2005.

[16] Bredmose, H. and N.G. Jacobsen, *Vertical Wave Impacts on Offshore Wind Turbine Inspection Platforms*, in *Proceedings of the ASME 2011 30th International Conference on Ocean, Offshore and Artic Engineering*2011, OMAE2011: Rotterdam, The Netherlands.

[17] Corte, C. and S.T. Grilli. *Numerical Modeling of Extreme Wave Slamming on Cylindrical Offshore Support Structures*. in *Proceedings of the Sixteenth International Offshore and polar Engineering Conference*. 2006. San Francisco, California, USA.

[18] Hu, Z.Z., et al., *Numerical simulation of floating bodies in extreme free surface waves.* Natural Hazards and Earth System Sciences, 2011. **11**: p. 519-527.

[19] Tromans, P.S., A. Anaturk, and P. Hagemeijer, *A new model for the kinematics of large ocean waves – application as a design wave.*, in *The Proceedings of the 1st International Offshore and Polar Engineering Conference*1991: Edinburgh, Uk. p. 64-71.

[20] Hunt-Raby, A.C., et al., *Experimental measurements of focused wave group and solitary wave overtopping.* Journal of Hydraulic Research, 2011. **49**(4): p. 450-464.

[21] Ransley, E., et al., *Numerical and physical modeling of extreme waves at Wave Hub*, in *Proceedings 12th International Coastal Symposium*, D.C. Conley, et al., Editors. 2013: Plymouth, England.

[22] Wave Hub. *About Wave Hub*. 2013 [cited 2013 March].

[23] Vyzikas, T., et al. *Integrated Numerical Modelling System for Extreme Wave Events at the Wave Hub Site*. in *Proceeding of ICE Conference: Coasts, Marine Structures and Breakwaters* 2013. Edinburgh, UK.

[24] Hunt, A., et al. *Kinematics of Focused Waves on a Plane Beach in the U.K. Coastal Research Facility*. in *Coastal Structures*. 2003. Portland, Oregon.

[25] Hirt, C.W. and B.D. Nichols, *Volume of fluid (VOF) method for the dynamics of free boundaries.* Journal of Computational Physics, 1981. **39**(1): p. 201-225.

[26] Jacobsen, N.G., D.R. Fuhrman, and J. Fredsøe, *A wave generation toolbox for the open-source CFD library: OpenFoam®.* International Journal for Numerical Methods in Fluids, 2012. **70**(9): p. 1073-1088.

[27] Sharma, J. and R. Dean, *Second-order directional seas and associated wave forces.* Society of Petrolium Engineers Journal, 1981: p. 129-140.

[28] Hunt, A., et al., *Phase inversion and the identification of harmonic structure in Coastal Engineering experiments*, in *Proceedings of the 29th International Conference on Coastal Engineering*, ASCE, Editor 2004: Lisbon, Portugal. p. 1047-1059.

[29] Zhao, X.Z., S.Z. C., and L.S. X., *A numerical study of the transformation of water waves in a wave flume.* Fluid Dynamics Research, 2009. **41**: p. 22.